Journal of Cell Science 111, 3597-3608 (1998)
Printed in Great Britain © The Company of Biologists Limited 1998
JCS4623

Myr 7 is a novel myosin IX-RhoGAP expressed in rat brain

Evelina Chieregatti*, Annette Gärtner‡, Hanns-Eugen Stöffler§ and Martin Bähler¶

Friedrich-Miescher Laboratorium in the Max-Planck Society, 72076 Tübingen and Adolf-Butenandt-Institut, Zellbiologie, Ludwig-Maximilians-Unversität, 80336 München, Germany

*Present address: Department of Anatomy and Cell Biology, Columbia University, College of Physicians and Surgeons, New York, NY 10032, USA

‡Present address: Max-Planck-Institute for Psychiatry, Am Klopferspitz 18a, D-82152 Martinsried, Germany

§Present address: EMBL Mouse Biology Programme, Adriano Buzzati-Traverso Campus, Via Ramarini 32, I-00015 Monterotondo, Italy

¶Author for correspondence at the Adolf-Butenandt-Institut (e-mail m.baehler@lrz.uni-muenchen.de)

Accepted 7 October; published on WWW 18 November 1998

SUMMARY

Rho family GTPases are important regulators of neuronal morphology, but the proteins directly controlling their activity in neurons are still poorly defined. We report the identification of myr 7, a novel unconventional myosin IX-RhoGAP expressed in rat brain. Myr 7 is a multidomain protein related to myr 5, the first class IX myosin to be characterized. It exhibits a myosin head domain with an N-terminal extension and a large insertion at loop 2, an actin contact site and regulator of myosin ATPase rate. The myosin head domain is followed by a neck domain consisting of six unevenly spaced consecutive IQ motifs representing light chain binding sites. The tail domain contains a C_6H_2-zinc binding motif and a region that specifically stimulates the GTPase-activity of Rho followed by a short stretch predicted to adopt a coiled-coil structure. Five alternatively spliced regions, one in the 5′-noncoding region, two in the myosin head and two in the tail domain, were noted. Analysis of myr 7 and myr 5 expression in different tissues revealed that myr 7 is expressed at high levels in developing and adult brain tissue whereas myr 5 is expressed only at moderate levels in embryonic brain tissue and at even further reduced levels in adult brain tissue. Myr 5 is, however, highly expressed in lung, liver, spleen and testis. Myr 7 is expressed in all brain regions and is localized in the cytoplasm of cell bodies, dendrites and axons. Myr 5 exhibits an overlapping, but not identical cellular distribution. Finally, a myr 7 fusion protein encompassing the GAP domain specifically activates the GTPase-activity of Rho in vitro, and overexpression of myr 7 in HtTA1-HeLa cells leads to inactivation of Rho in vivo. These results are compatible with a role for myr 7 (and myr 5) in regulating Rho activity in neurons and hence in regulating neuronal morphology and function.

Key words: Unconventional myosin, RhoGAP, Neuron, Rat

INTRODUCTION

Many cellular functions depend on the presence and dynamic organization of actin filaments. Actin filament organization and number are known to be regulated by various actin-binding proteins and signalling pathways. Recently, a growing number of unconventional myosins, molecular motors that produce directed force along actin filaments, have been identified. However, the functions of these unconventional myosins in actin-dependent processes remain largely to be determined. They were identified and classified as myosins based on conserved motor domain sequences. The myosin molecule myr 5 from rat and its human orthologue myosin-IXB define a ninth class of myosins (Reinhard et al., 1995; Wirth et al., 1996; Bähler et al., 1997). In addition to their myosin domain, they comprise a region that negatively regulates the activity of the Ras-related small G-protein Rho. Myr 5 stimulates the GTPase activity of Rho and thereby converts it from the active GTP-bound state to the inactive GDP-bound state (Reinhard et al., 1995; Müller et al., 1997). Rho activity has been shown to control actin organization and focal contact formation (Ridley and Hall, 1992). Therefore, these myosins are capable of regulating the organization of the actin filaments along which they might exert directed force. Several additional regions in myr 5 and myosin-IXB are noteworthy. They contain an N-terminal extension to their motor domain that probably exhibits a folding topology similar to the Ras-binding domains of Raf and Ral-GEF, but serves a different function, because it does not bind the monomeric G-protein Ras (Kalhammer et al., 1997). Within the myosin head domain in loop 2 (50/20 kDa junction) they contain a large insertion of more than hundred amino acids in length as compared to other myosins. In conventional myosin this loop 2 has been demonstrated to contact actin and to control the ATPase rates (Schröder et al., 1993; Uyeda et al., 1994). N-terminal to the Rho-GAP region in their tail domains, one finds a C_6H_2-zinc binding motif. Similar motifs are found in several signalling molecules such as protein kinase C, raf kinase and the proto-oncogene Vav (Reinhard et al., 1995). These motifs have been reported to bind lipids and proteins and to regulate kinase activity (Diaz-Meco et al., 1996; Mott et al., 1996).

Humans are likely to express a second class IX myosin molecule, because a short cDNA fragment encompassing a highly conserved region of the myosins head domain has been identified that is closely related to human myosin-IXB and rat

myr 5 (Bement et al., 1994). To get some insight into the conservation, structure-function relationships and potential redundancies of class IX myosins, we decided to determine the sequence of this novel putative class IX myosin from rat and to compare its tissue expression, cellular localization and GAP activity for different Rho-family members with that of myr 5.

MATERIALS AND METHODS

Cloning of myr 7

cDNA fragments of myr 7 and its human orthologue HuncM-IXA were amplified by 5′- and 3′-RACE. The HuncM-IXA fragment S1 (nucleotides 1-918; see Fig. 1) was amplified by two-step 5′-RACE PCR using human fetal liver 5′-RACE-Ready cDNA (Clontech, Palo Alto, CA), adaptor primer 1 and the two HuncM-IXA specific primers MB 200 (5′-TTCAACATAGGCACCAAGTACAG) and MB 199 (5′-AATCTGTTCTACTCCACTGGCAAA), which were deduced from the published partial HuncM-IXA sequence (Bement et al., 1994). The HuncM-IXA cDNA fragment HL4c1 (nucleotides 817-2424) was obtained by 3′-RACE PCR. Primary PCR was performed with human liver Marathon-Ready cDNA (Clontech) as a template and the adaptor primer 1 and the HuncM-IXA specific primer MB 211 (5′-TGAGCCCCACATTTATGCTGTGGCT). In a secondary PCR, HuncM-IXA specific primer MB 212 (5′-ATTTCAGG-AGAGAGTGGTTCTGGG) was used. Myr 7 cDNA fragments were amplified from rat spleen Marathon-Ready cDNA (Clontech). Fragments RM2a1/RM1a6 (nucleotides 1-1230) and RM1a3 (nucleotides 1-40, 337-1230) were generated by 5′-RACE PCR using adaptor primer 1 and specific primer MB 200 in the primary reaction and adaptor primer 2 and specific primer MB 199 in the secondary reaction. Fragment RM4a8 was derived from 3′-RACE PCR by primary amplification with primer pairs adaptor primer 1 and MB 211 followed by secondary amplification with primer pairs adaptor primer 2 and MB 212. PCR fragments were subcloned into pUC18 with the help of the SureClone ligation kit (Pharmacia Biotech, Freiburg) and completely sequenced. The RM4a8 fragment was used to screen 2×10^6 recombinant phages from a rat brainstem/spinal cord (27-29 day old rats) λ ZAP II cDNA library (Stratagene, La Jolla, CA). This screen yielded 22 positive clones. These clones were mapped by restriction analysis and sequenced at both ends. Clone B9 (nucleotides 58-1516, 1572-7459 and 7512-7716) was completely sequenced. Clone B11, which was missing a *Hin*dIII restriction site, was sequenced in the corresponding region to determine the missing nucleotides. To obtain clones encoding the C terminus of myr 7, the library was rescreened with an *Xba*I fragment of clone B9 (nucleotides 6916-7716). Of the 34 positive clones isolated, 12 clones were further analysed and clone B33 was completely sequenced. Clone B38 was overlapping with clone B33 and extended further to the 3′-end (nucleotide 6075-undetermined end). It was sequenced in the region overlapping with clone B33 and found to be identical. Sequencing of clone B43 at both ends revealed an insertion of 54 nucleotides when compared to clones B9, B33 and B38. All sequences were determined on both strands. Sequence analysis was performed using the GCG software package (Devereux et al., 1984). Amino acid sequences were investigated for their potential to adopt α-helical coiled-coil structures with the program Paircoil (Berger et al., 1995).

Northern blot analysis

A northern blot with poly(A)+ RNA (2 μg/lane) isolated from various rat organs was purchased from Clontech. The filter was prehybridized and hybridized at 42°C in 50% formamide, 5× SSC, 50 mM NaH_2PO_4, pH 7.0, 0.5% SDS, 0.1 mg/ml poly(A), 5 mg/ml denatured salmon sperm DNA and 5× Denhardt's reagent. The northern blot was probed for myr 7 mRNA with the S1 cDNA fragment (nucleotides 1-918) derived from human myosin-IXA. As a probe for myr 5 we used either a cDNA fragment spanning nucleotides 4820-5959 or nucleotides 5697-6088, which gave identical results. The cDNA probes were labeled using a random-primed DNA labeling kit (Boehringer, Mannheim, Germany). Following hybridization the filters were washed (2× SSC, 0.05% SDS at 50°C, 3× 15 minutes; 0.1× SSC, 0.1% SDS at 50°C, 2× 20 minutes), exposed to a storage phosphor screen and analyzed in a phoshorimager using the Image Quant software (Molecular Dynamics). For repeated use of the northern blot, the probes were removed by shaking the filter in 0.5% SDS at 95°C for 10 minutes.

Antibodies

To raise antibodies specific for myr 7, several fusion proteins were generated. PCR fragments encoding amino acids 718-853 (fusion protein 1), amino acids 1154-1345 (fusion protein 2) and amino acids 1408-1548 (fusion protein 3), respectively, were cloned into the *Bam*HI/*Hin*dIII restriction sites of the pQE30 6xHis-tag vector

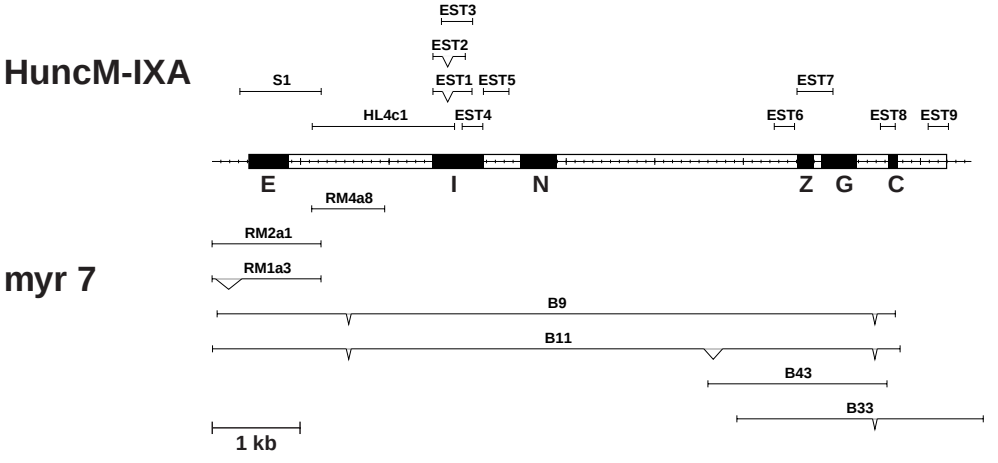

Fig. 1. Cloning and schematic representation of the overall structure of myr 7 and human myosin-IXA (HuncM-IXA). Human clones S1 and HL4c1 were derived from fetal liver cDNA by PCR amplification. Human expressed sequence tags EST1 (Accession No. D78714), EST2 (C17435), EST3 (C18070), EST4 (L48835), EST5 (H91407), EST6 (T05673), EST7 (T18954), EST8 (W00992) and EST9 (R22494) were discovered in a database search using the myr 7 sequence. Rat myr 7 clones RM2a1, RM1a3 and RM4a8 were derived from a rat spleen cDNA by PCR amplification. Clones B9, B11, B33 and B43 were derived from a rat brainstem cDNA library. Only a selection of isolated rat cDNA clones is indicated. Missing nucleotides in the differentially spliced clones are interrupted. In the schematic myr7 diagram the coding region is boxed. Shaded areas indicate the locations of the N-terminal extension (E), the loop 2 insertion (I), the neck region (N), the C_6H_2-zinc finger motif (Z), the GAP domain (G) and the predicted coiled-coil domain (C). The nucleotide sequence data are accessible through EMBL, GenBank, and DDBJ nucleotide sequence data bases under the accession numbers AJ 001713 (myr 7) and AJ 001714 (HuncM-IXA).

(Qiagen, Hilden, Germany). The fusion proteins were expressed in *E. coli* and purified under denaturing conditions over Ni-NTA-resin (Qiagen) as recommended by the supplier. Polyclonal antibodies against fusion protein 1 were raised in rabbit Tü 72, against fusion protein 2 in rabbits Tü 74, 75 and against fusion protein 3 in rabbits Tü 78, 79. The antibodies were affinity purified by standard techniques. Purified fusion proteins were coupled to CNBr-activated Sepharose-4B (Pharmacia) in 6 M urea, 0.1 M $NaHCO_3$, pH 8.0, according to the instructions of the manufacturer.

The polyclonal antibody Tü 66, which is directed against the C-terminal region of myr 5, was described previously (Reinhard et al., 1995). The monoclonal antibody FP3F8 directed against myr 5 was obtained by immunizing BALB/c mice with a C-terminal 6xHis fusion protein (amino acids 1851-1980) and subsequent fusion of splenocytes with the myeloma cell line Px.63.Ag8.653. Following cloning and selection, the hybridoma cell line FP3F8 was grown to confluence in 90% RPMI/10% FCS. Culture supernatant was collected and stored in 0.01% azide at 4°C. Monoclonal antibody 7.3b against synaptophysin was a gift of Dr Reinhard Jahn (Jahn et al., 1985).

Tissue preparation and immunoblotting

Tissues from rat were homogenized in 0.32 M sucrose, 5 mM Hepes, pH 7.4, and protein concentrations were determined by the method of Bradford (1976). Samples of the homogenates were immediately placed in SDS gel sample buffer (Laemmli, 1970) and boiled. Gel electrophoresis was performed according to Laemmli (1970) and immunoblotting according to Towbin et al. (1979). The blots were incubated with primary antibodies appropriately diluted in 5% nonfat dry milk/0.1% Triton X-100/TBS followed by peroxidase-coupled secondary antibodies diluted in the same buffer. The peroxidase reaction was visualized by the ECL system (Amersham Buchler, Braunschweig, Germany).

Preparation and immunostaining of tissue sections

Immunofluorescence staining of frozen rat brain and adrenal gland sections was performed as follows: rats were anesthetized with 7% chloralhydrate, transcardially perfused with PBS, followed by fixative consisting of 4% paraformaldehyde in PBS. Tissues were excised, equilibrated in 30% sucrose/PBS, moulded in Tissue Tek (Miles Inc., Elkhart, IN) and frozen in liquid nitrogen. Cryosections of 10 µm thickness were cut in a Frigo Cut (model 2700; Reichert und Jung, Nussloch/Heidelberg, Germany) at −20°C and adsorbed onto glass slides pretreated with 1% gelatin, 0.05% NH_4CrO_4. Sections were incubated for 1 hour at 37°C with primary antibodies appropriately

```
   1  MNVSDGGRRR FEDNEHTLRI YPGTISEGTI YCPIPARKNS TAAEVIDSLI  E
  51  NRLHLDKTKC YVLAEVKEFG GEEWILNPTD CPVQRMMLWP RMALENRLSG
 101  EDYRFLLREK NLDGSIHYGS LQSWLRVTEE RRRMMERGFL PQPQQKDFDD
 151  LCSLPDLNEK TLLENLRNRF KHEKIYTYVG SILIAINPFK FLPIYNPKYV
 201  KMYDNHQLGK LEPHIYAVAD VAYHAMLQRK KNQCIVISGE SGSGKTQSTN
 251  FLIHHLTALS QKGFASGVEQ IILGAGPVLE AFGNAKTAHN NNSSRFGKFI
 301  QVNYQETGTV LGAYVEKYLL EKSRLVYQEH NERNYHVFYY LLAGASEEER
 351  LAFHLKQPEE YHFLNQITKK PLRQSWDDYC YDSEPDCFTV EGEDLRHDFE
 401  RLQLAMEMVG FLPKTRRQIF SLLSAILHLG NISYKKKTYR DDSIDICNPE
 451  VLPIVSELLE VKEEMLFEAL VTRKTVTVGE KLILPYKLAE AVTVRNSMAK
 501  SLYSALFDWI VFRINHALLN SKDLEKDTKT LSIGVLDIFG FEDYENNSFE
 551  QFCINFANER LQHYFNQHIF KLEQEEYRTE GISWHNIDYI DNTCCINLIS
 601  KKPTGLLHLL DEESNFPQAT NQTLLDKFKH QHEENSYIEF PAVMEPAFII
 651  KHYAGKVKYG VKDFREKNTD HMRPDIVALL RSSRNAFVSG MTGIDPVAVF
 701  RWAVLRAFFR AVVAFREAGK RHIQRKSGHD DTTPCTILKS MDSFSFLQHP  I
 751  VHQRSLEILQ RCKEEKYSIT RKNPRTPLSD LQGMNTLNEK NQHDTFDIAW
 801  NVRTGIRQSR LPTNNTSLLD KDGIFANSAS SKLLERAHGI LTRNKNFRSK
 851  PVLPKHLLEV NSLKHLTRLT LQDRITKSLL HLHKKKKPPS ISAQFQVSLS
 901  KLMETLDQAE PYFVKCIRSN AEKLPLRFSD ALVLRQLRYT GMLETVRIRQ
 951  SGYSSKYSFQ DFVSHFHVLL PQHIIPSKFN IQDFFRKINI NPDNYQVGKT
1001  MVFLKEHERQ HLQDLLHQEV LRRIILLQRW FRVLLSRQQF LHLRQASVII
1051  QRFWRNYLNQ KQVRNAAVEK DAFIMASAAS LLQASWRAHL ERQRYLELRA  N
1101  AAVIIQQRWR ELCRRRHRAA TCIQSRWRGY RQSKKYKEQR NKIILLQSIY
1151  RGFRARQRYK ALKEERLKET KLEHGLAQIK TCGPLEIQGS DPSEWEDRSF
1201  ANRVKAIEEC KSVIESNRIS RESSMDFSKE SPDKQQERGR SQSGTDLQGD
1251  VIVRQRPKSL EDLHQKKVGR AKRESRRMRE LEQAIFSLEL LKVRSLGGMS
1301  PSEERRWSTE LMPEGLQSPQ GTPDSESSQG SLELLTCDEN QKSKPESLIL
1351  DDGELKISSP STFTNPKFDS QNNALSASSE TSSTFSGKGA SSDSEHLKNG
1401  TAEEKLVYSS QPITCKSQLR DSFVSSSLPT FFYIPHQEPL KTSSQLDTSI
1451  QRNKLPERET TLKTTLTLDI NREARKCQFS GQVTPLNPDS SCTVLKKLEK
1501  LNIEKEKRQK QLQQQNEKEM MEQIRQQTDI LEKERKAFKT IEQSRTEASL
1551  LAPSFYQSRQ KVERPSSLHI QNTPSKGEAG VLGSPSALAT KDSPSIHLPP
1601  KDRPVTLFFE RKGSPCQSRT VKELTKTERM GTQHDAACRL SNNHNTEREH
1651  FKSTHSYSHR SDDPSREGSS RPIFFTPKDN VITPLVHSGN PQVHKQDEPA
1701  WKSKLAGPGQ REVARPAHKK KARMARTRSD FLTRGTFADG EGDTEEDDYD
1751  DIIEPLLSLD QASHSELGPV SSLGQASHSD SEMTSQRFSS VDEQARLHKA
1801  MSQGEITKLA GRQKSSDLDI RPQRAKMRFW AKGKQGEKKT TRVKPAPQSE
1851  VSSLFAGSDV TPVHPFSDEL TQYHPTPPLS PELPGSCRKE FKENKEPSPK
1901  AKRKRGVKIS SVALDSMHWQ NDSVQIIASA NDLKSMDEFL LKKMNDLDNE
1951  DSKKDTLVDV VFKKALKEFR QNIFSSYSSA LAMDDGKSIR YKDLYALFEQ
2001  ILEKTMRFEQ RDWNESPVRV WVNTFKVFLD EYMNEFKTLD STAPKVLKTE
2051  RKKRRKKETD LVEEHNGHMF KATQYSIPTY CEYCSSLIWI MDRASVCKLC  Z
2101  KYACHKKCCL KTTAKCSKKY DPELSSRQFG VELSRLTSED RAVPLVVEKL
2151  INYIEMHGLY TEGIYRKSGS TNKIKELRQG LDTDAESVNL DDYNIHVIAS  G
2201  VFKQWLRDLP NPLMTFELYE EFLRAMGLQE RKETIRGVYS VIDQLSRTHL
2251  STLERLIFHL VRIALQEDTN RMSANALAIV FAPCILRCPD TTDPLQSVQD
2301  ISKTTTCVEL IVVEQMNKYK ARLKDISSLE FAENKAKTRL SLIRRSMKPV
2351  LIAVRFMSIT RSSVSGKGRL HRGSHPNPSS PVIVRLPSMS DVPEETLTSE
2401  TAMDTDVTDQ QQAAMQQEEK VLTEQIENLQ KEKEELTFEM LVLEPRASDD  C
2451  EALESEASIG TADSSENLNM DPEERSLALS SLKAAGKSEP SSKFRKQLRK
2501  QPDSLDSVSS SVSSCLSNTT SSHGTRKRFQ IYSKSPFYRA ASACEAQGME
2551  GPLGQAKSLE DRPQFISRGT FNPEKGKQKL KNVKNSPQKT KETPEGTVSS
2601  GRKKTVDSDC SSTQQLPLFG NNEFMV
```

Fig. 2. The deduced amino acid sequence of myr 7 (amino acids 1-2626) is shown in single-letter code. The N-terminal extension (E) preceding the conserved myosin head sequences, the large insertion at loop 2 (I), the six putative light chain binding IQ-motifs (N; conserved IQ residues in bold) and the sequence homologous to Rho family GTPase-activating proteins (G) are boxed. The zinc ion coordinating residues of the C_6H_2-motif (Z) are highlighted on a black background. The sequence predicted to form a coiled-coil structure (C) is shown in bold. Alternatively spliced sequences are underlined.

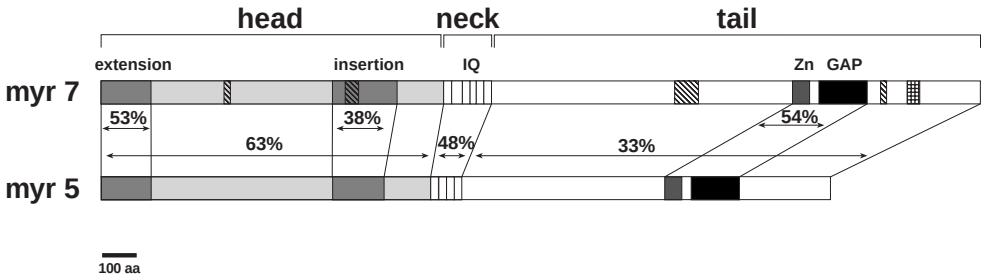

Fig. 3. Schematic diagram comparing myr 7 and myr 5 myosin head, neck and tail domains. Amino acid sequence identities (%) between corresponding regions and motifs are given. The region predicted to adopt a coiled-coil structure in myr 7 is square-hatched. The alternatively spliced regions are cross-hatched. IQ denotes the IQ-light chain binding motifs, Zn denotes the C_6H_2-zinc binding region and GAP denotes the Rho family GTPase-activating protein motif.

diluted in 5% normal goat serum in PBS. Following several wash steps, the sections were incubated for 30 minutes at 37°C with secondary goat anti-rabbit antibodies coupled to FITC and goat anti-mouse antibodies coupled to Lissamine rhodamine (Dianova, Hamburg, Germany). After three wash steps with PBS, sections were mounted in 15% Mowiol 4-88 (Hoechst, Frankfurt, Germany), 30% glycerol in PBS, pH 8.0.

Alternatively, the staining procedure was performed on free-floating cryotome sections (60 μm in thickness). Sections were incubated with primary antibodies appropriately diluted in 5% normal goat serum in PBS and either with or without 0.1% Triton-X-100 for 2 hours at room temperature, followed by peroxidase-coupled secondary antibodies diluted in the same buffer for 1 hour at room temperature. The peroxidase-labelled antibodies were visualized by preincubating the sections for 10 minutes in 3,3′-diaminobenzidine (700 μg/ml, Sigma, St Louis, MO) before starting the reaction by the addition of 0.01% H_2O_2. After 5-10 minutes the reaction was stopped with several washes in PBS; the sections were dehydrated overnight and then mounted onto gelatinized slides together with coverslips and Entellan (Merck, Darmstadt, Germany).

Immunofluorescence labeling of cells grown in culture

HtTA-1 HeLa cells were cultured on coverslips as described (Müller et al., 1997) and fixed in 4% paraformaldehyde/PBS. After quenching with 0.1 M glycine/PBS, the cells were permeabilized for 20 minutes in 0.1% saponin, 5% normal goat serum, PBS. Primary and secondary antibodies were appropriately diluted in 5% normal goat serum/PBS. Secondary goat anti-rabbit antibody coupled to Lissamine rhodamine was purchased from Dianova, FITC-coupled phalloidin was from Molecular Probes Inc. (Eugene, OR). Cells were rinsed with PBS and mounted as described above.

Hippocampal neurons were prepared from E17 Wistar rat embryos according to the protocol of Zafra et al. (1990). Briefly, hippocampi were incubated for 20 minutes at 37°C in PBS containing 10 mM glucose, 1 mg/ml BSA, 1 μg/ml DNase and 5 mg/ml papain, dissociated mechanically with a pasteur pipette and plated in DMEM/10% FCS on poly(D,L)ornithine-coated 10 mm glass coverslips at a density of 5×10^4 cells. The medium was changed after 2 hours to defined medium. For labeling of cells by indirect immunofluorescence they were fixed with 4% paraformaldehyde in PBS for 20 minutes, permeabilized with 0.2% Triton X-100, and quenched with 0.1 M glycine for 20 minutes and 20% goat serum for 1 hour. The cells were incubated overnight with the myr 7 antibody Tü 78 (50 μg/ml), washed and incubated for 1 hour with a goat anti-rabbit antibody coupled to Lissamine rhodamine. The antibodies were diluted in 1% goat serum in PBS. Cells were analyzed by confocal microscopy (Leica, Heidelberg, Germany). The thickness of the optical sections varied between 80 nm and 150 nm. Maximal intensity projections of the stack of optical sections were calculated using the program image space (Molecular Dynamics).

Determination of GAP activity

The myr 7 cDNA fragment encoding the GAP domain (amino acids 2144-2287) was amplified by PCR and inserted into *Bam*HI and *Xho*I restriction sites of the pGEX-4T-3 GST expression vector (Pharmacia). The GST-myr 7 GAP domain fusion protein expressed in *E. coli* was insoluble and present in inclusion bodies. To extract the

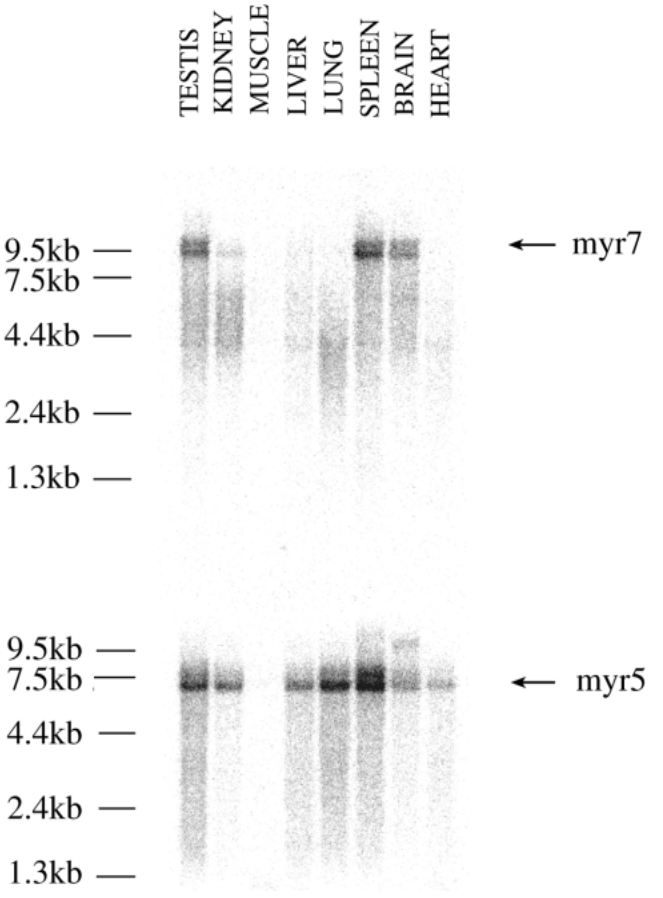

Fig. 4. Northern blot analysis of myr 7 and myr 5 mRNA in adult rat tissues. The northern blots were hybridized with the HuncM-IXA PCR fragment S1, nucleotides 1-918 (upper panel) or with a myr 5 fragment, nucleotides 5697-6088 (lower panel). The positions of myr 7 and myr 5 mRNA are indicated on the right, size standards on the left. The respective rat tissues are indicated above each lane.

protein from the inclusion bodies, the washed cell pellet was solubilized for 1 hour in a buffer of 8 M urea, 50 mM Tris-HCl pH 7.5, 1 mM EDTA, 1 mM DTT as described by Ahmed et al. (1995). The protein was refolded by removing urea in a two-step dialysis procedure: the protein sample (5 ml) was first dialysed for 1 hour against 500 ml of 4 M urea, 1 mM Tris-HCl, pH 5.0, 1 mM DTT, followed by overnight dialysis against 2 l of 50 mM Tris-HCl, pH 7.5, 50 mM NaCl, 2 mM $MgCl_2$, 200 μM DTT with two changes of buffer. The suspension was clarified by centrifugation (10,000 ***g*** for 30 minutes, 4°C) and the supernatant was incubated with glutathione-Sepharose 4B (Pharmacia) for 2 hours at 4°C, washed and the bound protein eluted with 5 mM glutathione, 50 mM Tris, pH 8.0.

Recombinant small GTPases were expressed as GST fusion proteins and obtained in purified form after thrombin cleavage as described (Ridley et al., 1992). GTPase assays were carried out as described by Settleman and Foster (1995).

Plasmid construction and transfection of HtTA-1 HeLa cells

The myr 7 cDNA encoding an additional C-terminal haemagglutinin (HA) epitope was assembled and cloned into the pUHD10-3 expression vector. The HA-epitope encoding sequence was added by PCR using an oligonucleotide containing a *Cla*I site followed by nucleotides 6778-6801 of myr 7 as a 5′-primer and an oligonucleotide containing nucleotides 8275-8297 of myr 7, the HA-epitope encoding sequence, a stop codon and a *Not*I site as a 3′-primer. Clone B33 served as a template. The amplified fragment was subcloned into pBSK+ from where it was cut out again by *Rca*I/*Not*I. It was ligated into the *Xho*I/*Not*I sites of the pBSK+ vector together with a *Xho*I/*Rca*I fragment of clone B9, which comprises the remaining myr 7 sequence. The complete myr 7-HA cDNA was then subcloned into the pUHD10-3 vector as follows: myr 7 pBSK+ was first digested with *Not*I, made blunt with Klenow polymerase and then digested with *Sac*II. This fragment was ligated to the *Sac*II and to the blunted *Xba*I sites of the pUHD10-3 vector. The arginine in the GAP domain at position 2166 was mutated to a methionine by using the Quick Change mutagenesis kit (Stratagene). Introduction of the mutation was verified by sequencing.

HtTA-1 HeLa cells were cultured in DMEM supplemented with 10% fetal calf serum, 2 mM L-glutamine, 0.1 mg/ml streptomycin/penicillin and 400 μg/ml active G-418 sulphate (Gibco BRL, Gaithersburg, MD). Cells were transfected with the plasmid myr 7-HA pUHD10-3 using calcium phosphate precipitation (Ausubel et al., 1989). As a control, cells were mock transfected with pUHD10-3 vector alone.

RESULTS

Cloning of myr 7 cDNA reveals that it encodes a myosin-RhoGAP related to myr 5/myosin-IXB

We used the limited sequence information available for human myosin-IXA (Bement et al., 1994) to obtain partial cDNA clones from human and full-length cDNA clones encoding the orthologue from rat, called myr 7 (seventh **my**osin from **r**at)

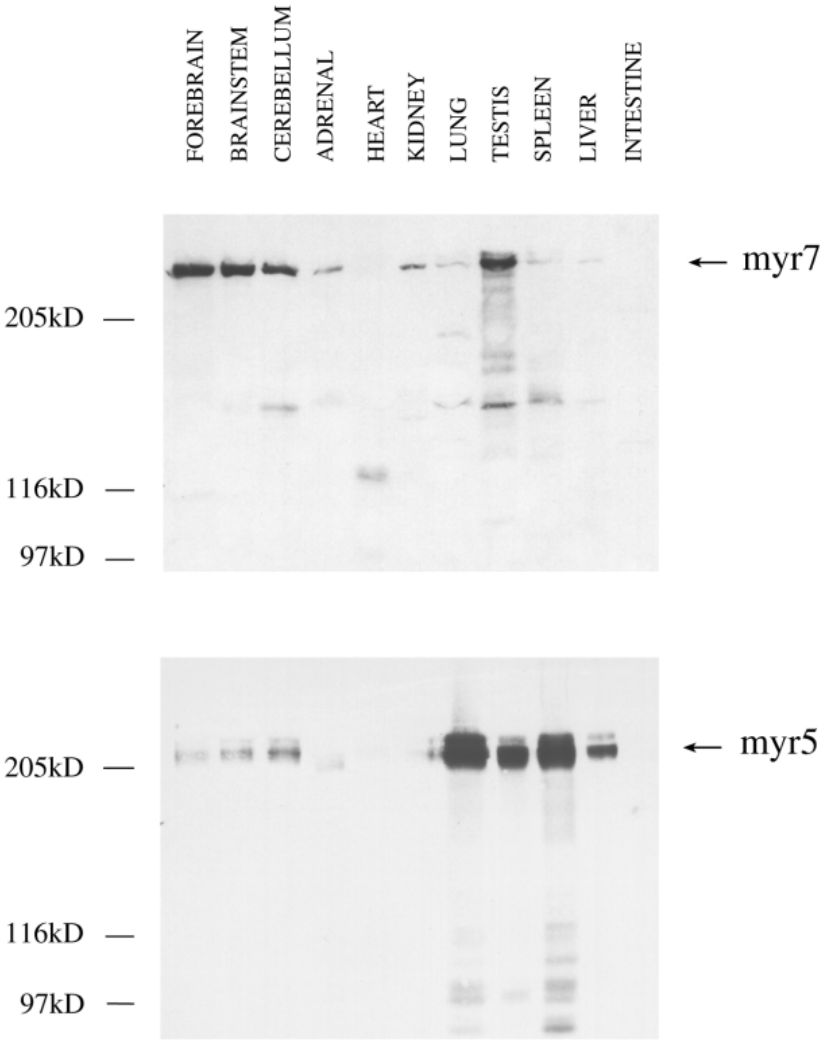

Fig. 5. Tissue distribution of myr 7 and myr 5. Equal amounts (100 μg) of protein from the different tissues and brain regions were separated by SDS-PAGE and immunoblotted with the affinity purified myr 7 antibody Tü 74 (upper panel) and the monoclonal myr 5 antibody FP3F8 (lower panel) followed by secondary antibody coupled to peroxidase. The peroxidase reaction was visualized with the ECL system (Amersham). The positions of myr 7 and myr 5 are indicated on the right. Positions of molecular mass standards are shown on the left. Tissues and brain regions are indicated on top of each lane.

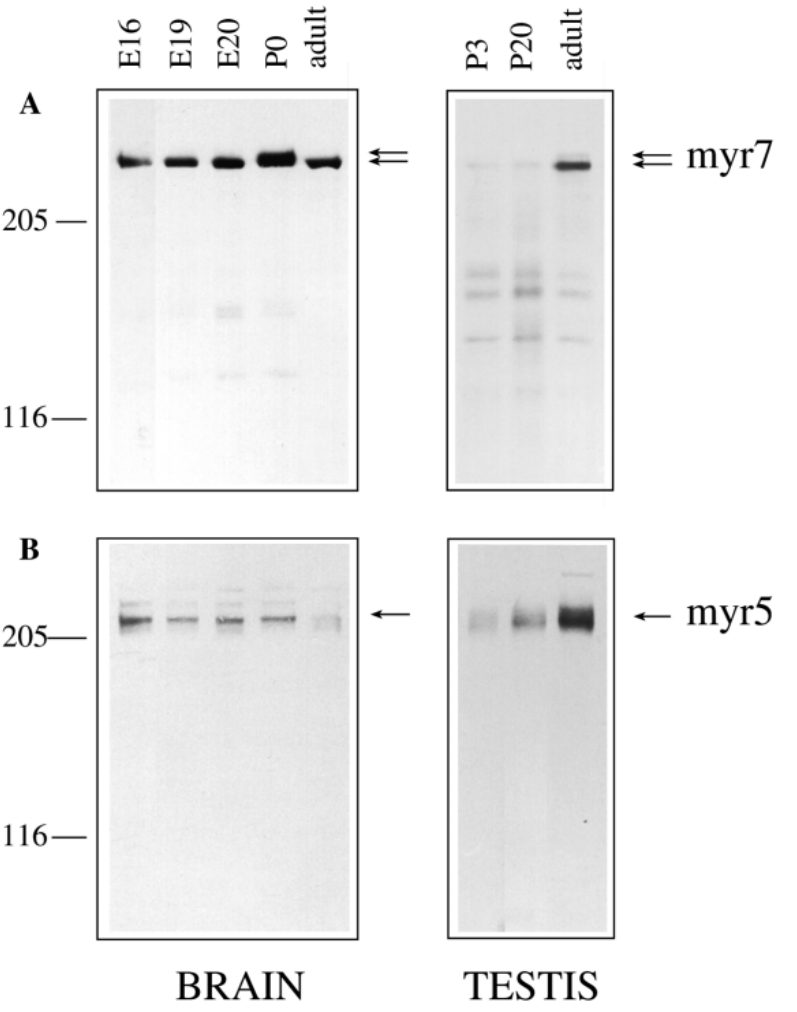

Fig. 6. Developmental expression of myr 7 and myr 5 in brain and testis. Equal amounts (100 μg) of protein from brain (left panels) and testis (right panels) homogenates derived from rats of different embryonic (E) and postnatal (P) stages were separated by SDS-PAGE and immunoblotted with myr 7 antibody Tü 74 (A) or with myr 5 antibody FP3F8 (B), followed by secondary antibody coupled to peroxidase. The positions of myr 7 and myr 5 are indicated on the right. Molecular mass standards in kDa are shown on the left. Developmental age is given on top of each lane and the tissue is indicated below the panel.

(Fig. 1). The complete cDNA sequence of myr 7 was assembled from various overlapping clones isolated from a rat brainstem/spinal cord cDNA library. The assembled cDNA, which included several alternatively spliced regions, was 8575 nucleotides in length and encoded a protein of 2626 amino acids with a predicted molecular mass of 301,379 kDa (Fig. 2). In its 5′-non-coding region myr 7 exhibited a differentially spliced region of 297 nucleotides (Fig. 1), the functional significance of which is unclear. Analysis of the deduced myr 7 amino acid sequence revealed that it encodes a myosin head domain (amino acids 1-1021), a neck region with six putative light chain binding sites (amino acids 1022-1163) and a tail domain (amino acids 1164-2626) that contains a C_6H_2-zinc ion binding motif followed by a region with homology to GTPase-activating proteins for the Rho family of small G-proteins (Rho-GAPs) (Figs 2, 3). Alignments of the myr 7 myosin head domain with the head domains of other myosin molecules demonstrated that, together with myr 5 and human myosin-IXB, myr 7 forms a distinct ninth class of myosin molecules (data not shown). Its myosin head domain contains all the sequences typical for myosin molecules. Additionally, like myr 5/human myosin-IXB, it contains an N-terminal extension preceding its myosin head domain and a large insertion in the loop 2 (50/20 kDa junction in myosin-II) of the myosin head domain, which in

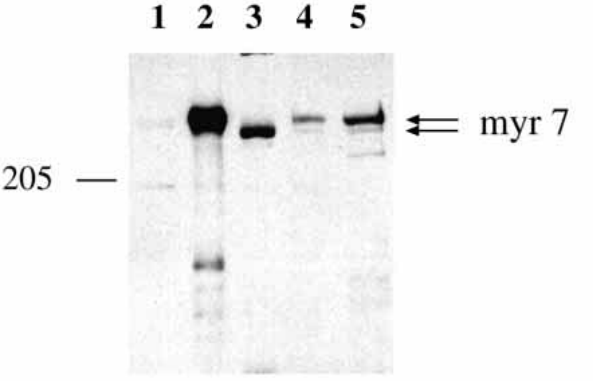

Fig. 7. Detection of myr 7 protein bands with different electrophoretic mobilities. Proteins of HeLa cells and rat tissue homogenates were separated by SDS-PAGE and immunoblotted with myr 7 antibody Tü 72, raised against a fusion protein encompassing amino acids 699-834, followed by secondary antibody coupled to peroxidase. The myr 7 protein bands are indicated on the right. Molecular mass standard in kDa is denoted on the left. Proteins from the following cells and tissues were separated: HeLa cells, 100 μg (lane 1); HeLa cells transfected with pUHDmyr 7-HA plasmid, 20 μg (lane 2); adult rat brain, 50 μg (lane 3); adult rat adrenal gland, 100 μg (lane 4) and adult rat spleen, 120 μg (lane 5).

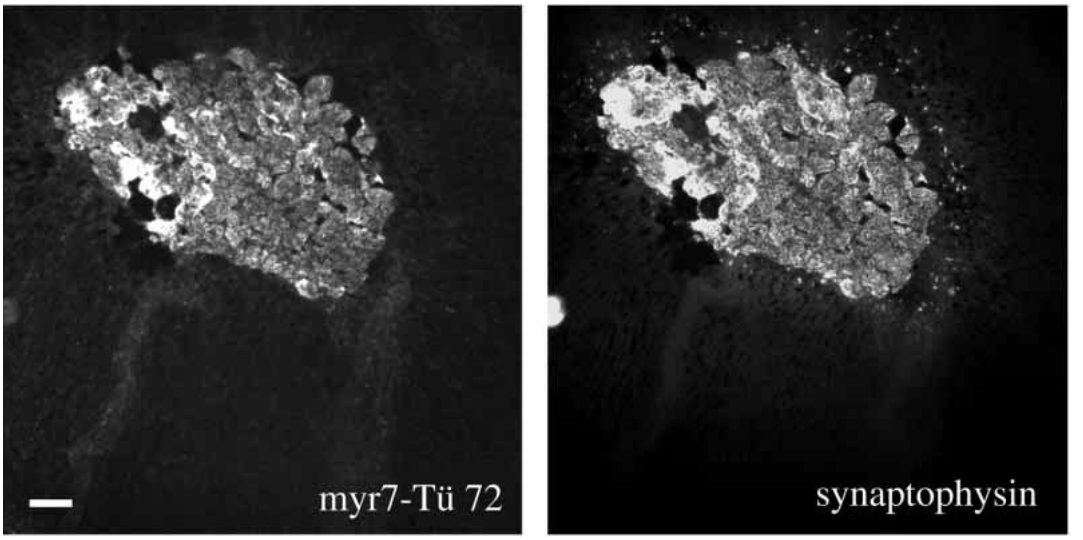

Fig. 8. Immunolocalization of myr 7 in rat adrenal gland. Cryosections of adrenal gland were labeled by indirect immunofluorescence with the myr 7 antibody Tü 72, followed by a FITC-coupled goat anti-rabbit antibody. The same sections were double stained with a monoclonal synaptophysin antibody followed by a Lissamine rhodamine-coupled goat anti-mouse antibody. The medullary part only of the adrenal gland is stained by synaptophysin and by Tü 72. Bar, 100 μm.

myosin-II has been implicated in actin binding. The N-terminal extension of myr 7 is 53% identical (59% similar) to the N-terminal extension of myr 5 (Fig. 3). It was suggested that this domain in myr 5 represents a Ras-binding domain (Ponting and Benjamin, 1996). However, we showed that this domain in myr 5 is not a Ras-binding domain, although it is likely to exhibit a folding topology similar to bona fide Ras-binding domains (Kalhammer et al., 1997). Similarly, the N-terminal extension of myr 7 is not able to bind Ras (G. Kalhammer and M. Bähler, unpublished observations). The large insertion in the loop 2 region previously only found in the myr 5/HuncM-IXB myosin head regions is also found in myr 7 and is even 46 amino acids longer than the insertion of myr5/HuncM-IXB. Database searches with the myr 7 sequence identified four expressed sequence tags of human origin covering the region of the loop 2 insertion of the homologous myosin-IXA (Accession No. D78714, C17435, C18070, L48835). Interestingly, two of the EST sequences lacked 40 amino acid residues as compared to the myr 7 sequence (amino acids 2602-2721 in myr 7), whereas one of the EST sequences and our partial human cDNA were identical in length to the myr 7 sequence. This finding demonstrates that a region of 40 amino acids within the insertion in the human head sequence can be alternatively spliced. Myr 7 exhibits in its head domain as a splice variant

Fig. 9. Immunolocalization of myr 7 in adult rat brain. Sagittal cryosections of perfused rat brain were stained with myr 7 antibody Tü 78 (A,B) or Tü 74 (C,D) followed by peroxidase-coupled secondary antibody. (A) Overview of a complete sagittal rat brain section; (B-D) higher magnifications of the cerebellar foldings (B); the CA3 region of the hippocampus (C) and the layer 5 in the cortex (D).

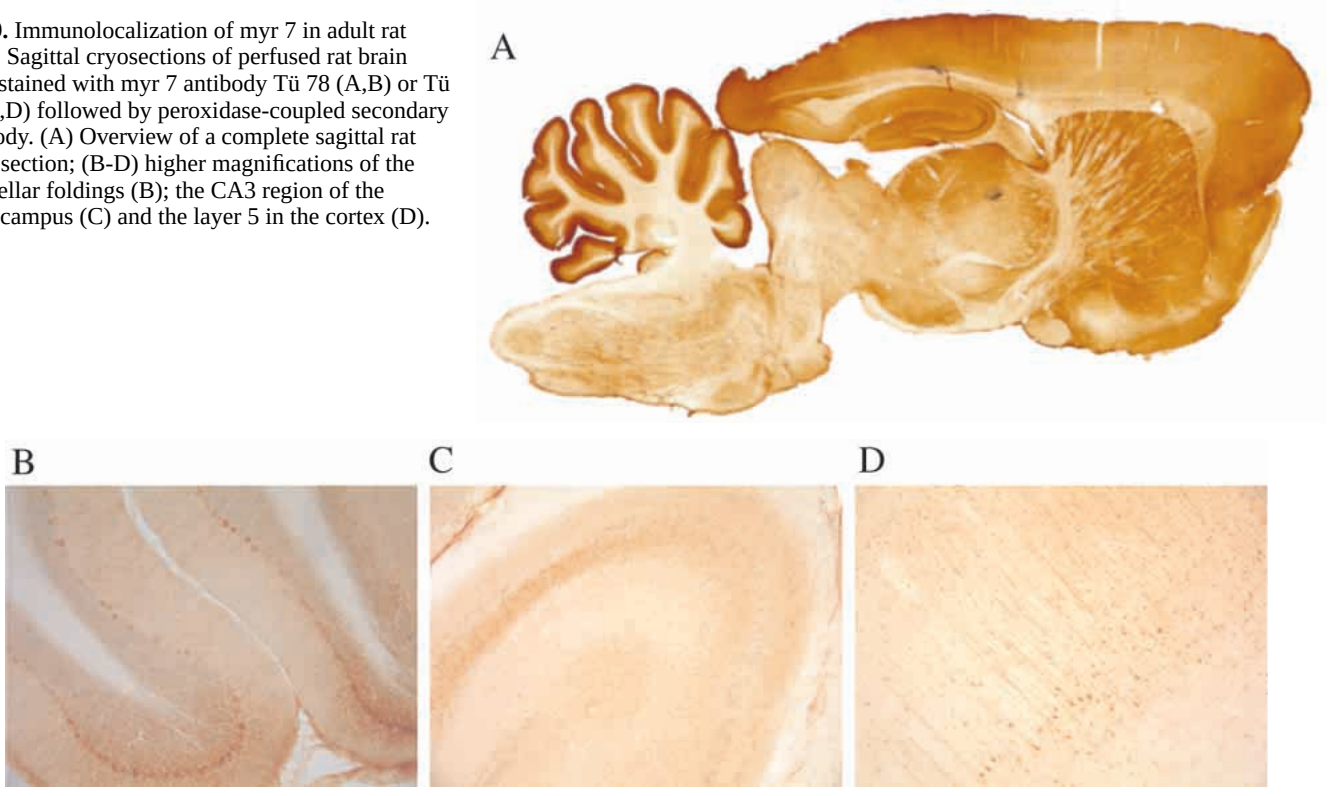

another insertion of 19 amino acids (amino acids 367-385) at a position where class-VI myosins were also found to have an insertion in comparison to the other known myosin molecules.

The neck region contains six putative light chain binding IQ-motifs. IQ-motifs 1, 3, 5 and 6 are 23 amino acids in length. Between the second and third IQ-motif there is an insertion of an extra nine amino acids and the fourth IQ-motif is 5 amino acids shorter and therefore only 18 amino acids in length.

Just as the myr 5 tail domain, the myr 7 tail domain contains a C_6H_2-zinc ion binding motif followed by a region with similarity to Rho-family GTPase activating proteins (Figs 2, 3). However, the myr 7 tail domain is considerably longer than the myr 5 tail domain. The region between the neck domain and the C_6H_2-motif is not particularly well conserved in sequence between the two myosins, but exhibits a similar amino acid composition. The C_6H_2-motif and the region with similarity to Rho-GAP proteins share 54% sequence identity with the corresponding regions in the myr 5 tail domain (Fig. 3). The C-terminal region of myr 7 is about 150 amino acids longer than in the myr 5 tail domain and contains a short region (amino acids 2408-2444) that is predicted by the program paircoil (Berger et al., 1995) to adopt a coiled-coil structure. The analysis of different cDNA clones revealed two alternatively spliced regions within the myr 7 tail domain: a longer region encoding 71 amino acids (amino acids 1713-1783) and a shorter region encoding 18 amino acids (amino acids 2348-2365).

Tissue distribution and developmental regulation of myr 7 and myr 5

We investigated the expression of both myr 7 mRNA and protein in various rat tissues and compared it with the expression of myr 5. Northern blot analysis of poly(A)$^+$ RNA from adult rat tissues revealed a doublet of myr 7 mRNA bands with apparent sizes of 9.5 and 10.5 kb, respectively. This doublet was detected in brain, testis, spleen and, with considerably reduced abundance, in kidney (Fig. 4, upper panel). The myr 5 transcript migrated as a broad band with an apparent size of 7 kb. In comparison to myr 7, myr 5 mRNA exhibited a more widespread tissue distribution and was detected in testis, kidney, liver, lung, spleen, brain and heart muscle (Fig. 4, lower panel). In brain tissue, an additional minor band of approximately 10 kb in size was detected.

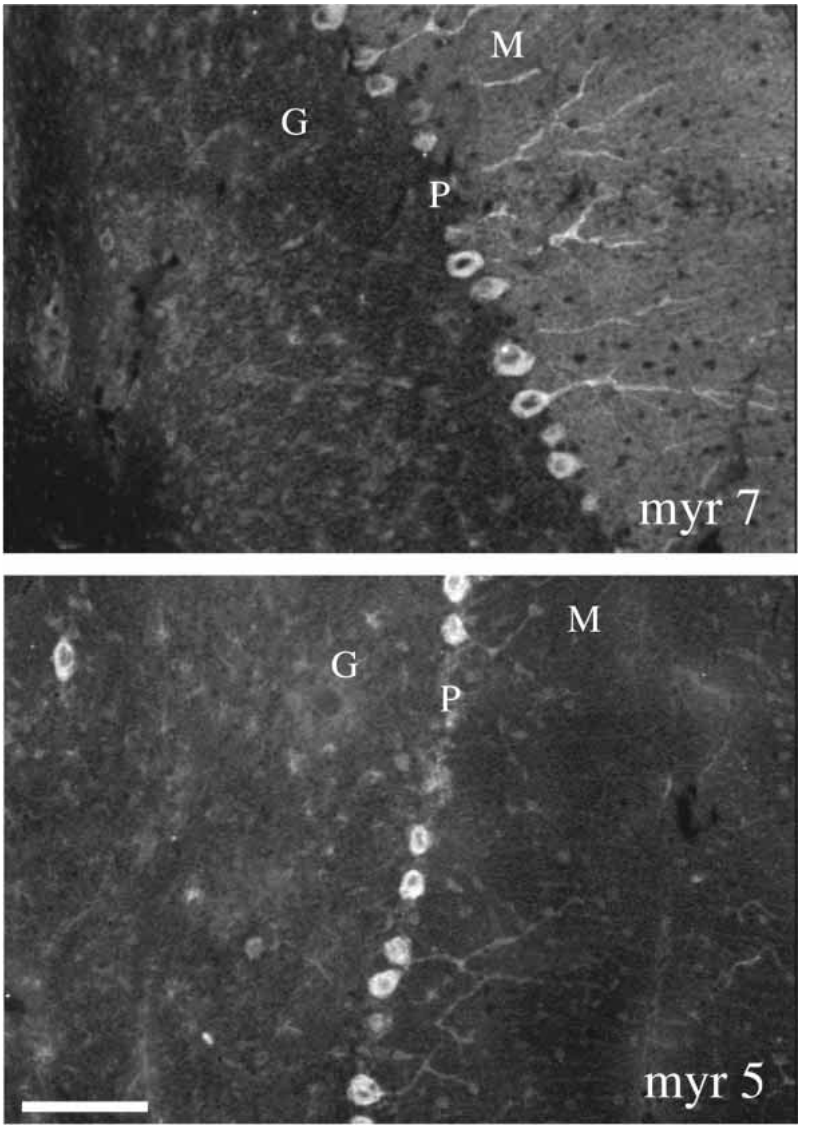

Fig. 10. Immunolocalization of myr 7 and myr 5 in the adult rat cerebellum. Sagittal cryosections of the cerebellum were stained with myr 7 antibody Tü 78 and myr 5 antibody Tü 66, respectively, followed by a FITC-coupled goat anti-rabbit antibody. G, granular layer; P, Purkinje cell bodies; M, molecular layer. Bar, 100 μm.

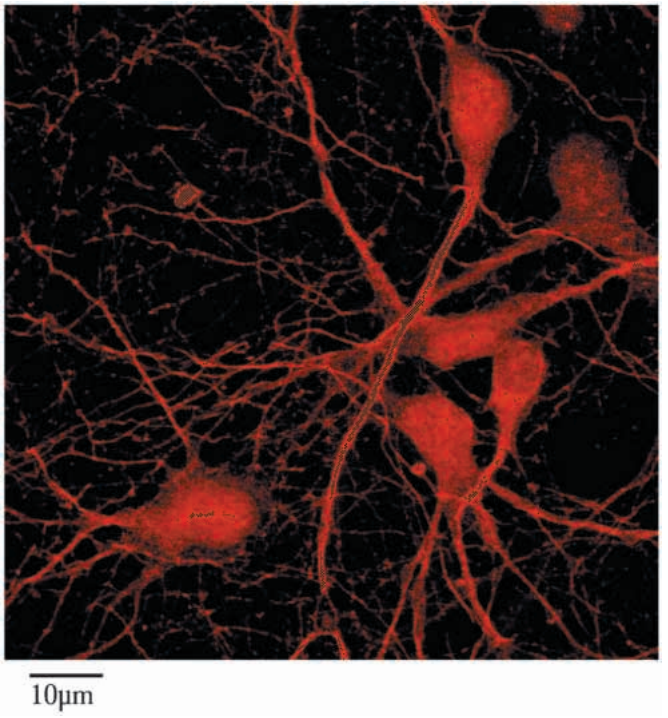

Fig. 11. Immunolocalization of myr 7 in primary hippocampal neurons in culture. Cells were stained with myr 7 antibody Tü 78 followed by Lissamine rhodamine-coupled secondary antibody and viewed in a confocal microscope. Shown is a composite of six consecutive optical sections of 86 nm thickness.

Antibodies raised against fusion proteins encompassing various regions of myr 7 specifically recognized a protein with a molecular mass of 300 kDa on immunoblots (Fig. 5). This molecular mass is in excellent agreement with the deduced molecular mass of 301 kDa from cDNA cloning. The myr 7 protein was most abundant in brain and testis and lower levels were also detected in adrenal gland, kidney, lung and spleen (Fig. 5, upper panel). The myr 5 protein was abundant in lung, testis, spleen and liver and reduced levels were detected in different brain regions (Fig. 5, lower panel).

Myr 7 and myr 5 protein expression is developmentally regulated. During rat forebrain development, myr 5 is expressed at higher levels in embryonic and early postnatal stages than in the adult forebrain (Fig. 6B). As opposed to myr 5, the myr 7 protein levels increased somewhat during embryonic development of the forebrain (Fig. 6A). However, in embryonic and early postnatal days a slightly slower migrating form of myr 7 was observed than in the adult, indicating that there is a developmental switch in myr 7 isoform expression. Analysis of myr 7 and myr 5 expression in maturing (postnatal days 3 and 20) and adult testis demonstrated that both proteins are expressed at lower levels in the immature testis as compared to the adult testis (Fig. 6), implying a function in germ cell maturation.

Antibodies against myr 7 detect differentially expressed protein bands

Upon comparison of myr 7 protein expression in different tissues, we noted that two closely spaced bands were recognized by our myr 7 antibodies (Fig. 7). In adult brain tissue a single protein band was detected. This band exhibited a slightly faster migration on SDS-PAGE than the major band recognized in adrenal and spleen. However, in both of these tissues a less prominent faster migrating band was also detected. Transfection of myr 7 cDNA assembled from clones B9 and B33 into HeLa cells lead to the expression of the slower migrating band. In non-transfected HeLa cells a very faint band of identical molecular mass to the expressed myr 7 protein was detected. Although the exogenously expressed myr 7 contained a C-terminal HA-epitope, it appears unlikely that the slower migration is simply due to this epitope-tag. A likely explanation for the observed variability of electrophoretic mobilities is that they correspond to alternatively spliced forms of myr 7. However, alternative explanations cannot be excluded.

Distribution of myr 7 immunoreactivity in adrenal gland and brain

We determined the localization of myr 7 in adrenal gland and adult rat brain. Immunofluorescence labeling of adrenal gland cryosections with myr 7 antibodies revealed a selective expression of myr 7 in the medulla but not in the cortex, as visualized by double-immunofluorescence with an antibody against synaptophysin, an integral membrane protein of secretory vesicles (Fig. 8).

Staining of sagittal sections of adult rat brain with antibody Tü 78 demonstrated a widespread distribution of myr 7 in the brain (Fig. 9A). Elevated levels of myr 7 immunoreactivity were detected in the cerebellum, in two layers of the cortex and in the dentate gyrus and the CA2-CA3 regions of the hippocampus. Analysis of the subcellular localization of myr 7 in different brain regions revealed an enrichment of myr 7 in cell bodies and dendrites. In the cerebellum myr 7 immunoreactivity was prominent in the molecular layer, especially in cell bodies and apical dendrites of Purkinje cells. Staining was also noticed in the cell bodies and dendrites of granule cells (Figs 9B, 10A). A similar subcellular distribution of myr 7, namely in cell bodies and dendrites, was observed in the CA3 layer and in the dentate gyrus of the hippocampus (Fig. 9C). In the cortex myr 7 was enriched in cell bodies and dendrites of pyramidal cells in layers 3 and 5 (Fig. 9D). A comparison of myr 7 and myr 5 distribution revealed a considerable overlap between the two proteins, but also some differences. Whereas the molecular layer in the cerebellum was brightly stained with myr 7 antibodies, it was hardly stained at all with myr 5 antibodies (Fig. 10). Both molecules were detected in the cell bodies and apical dendrites of Purkinje and granule cells.

In hippocampal cells in culture myr 7 immunofluorescence was distributed throughout the cells (Fig. 11). Cell bodies, dendrites and axons were labelled. The staining appeared to be mostly cytoplasmic, with occasional hints of an enrichment near the plasma membrane.

Myr 7 activates specifically the GTPase activity of Rho

To test whether the region in the myr 7 tail domain with homology to Rho family GAPs was capable of stimulating GTP hydrolysis of Rho family members, we expressed this region as a glutathione S-transferase fusion protein in *E. coli*. The refolded, purified GST-myr 7 GAP region was tested for its GAP activity on recombinant RhoA, Rac1 and Cdc42Hs. The myr 7 GAP region stimulated GTP-hydrolysis of RhoA (Fig.

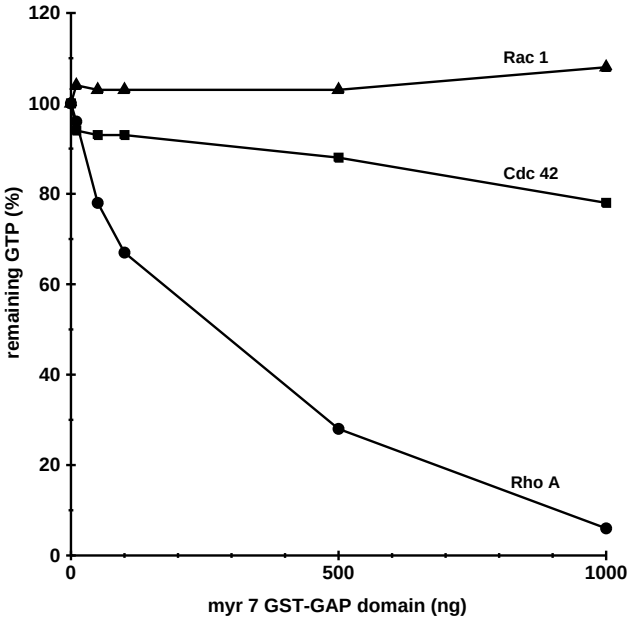

Fig. 12. GAP activity of GST-myr 7 GAP domain fusion protein on RhoA, Rac1 and Cdc42. Increasing amounts of purified, refolded GST-myr 7 GAP domain were incubated for 15 minutes with 0.1 μg Rho family GTPases preloaded with [γ-^{32}P]GTP. The remaining GTPase-bound radioactive GTP was determined in a filter binding assay. Remaining GTP in control assays without any addition of GST-myr 7 GAP domain was set 100%.

12) and of RhoB. It was only marginally active on Cdc42Hs and not at all on Rac1 (Fig. 12). These results demonstrate that in vitro the myr 7 GAP region acts as a Rho-GAP. To test for in vivo Rho-GAP activity of myr 7, we overexpressed myr 7 tagged at its C terminus with a haemagglutinin-epitope in HtTA-1 HeLa cells. Cells overexpressing myr 7 exhibited an altered morphology and actin filament organization (Fig. 13). They were rounded up and showed numerous extensions, whereas cells not transfected were well spread. In cells transfected with myr 7, actin filaments were no longer organized in stress fibers and peripheral bundles, but instead appeared fragmented and accumulated in the perinuclear region. These cellular alterations were due to the Rho-GAP activity of overexpressed myr 7. Inactivation of the Rho-GAP activity of myr 7 by mutation to a methionine of a conserved arginine residue in the Rho-GAP domain (residue 2166), which has been demonstrated to be essential for catalysis of GTP hydrolysis by other Rho-GAPs (Müller et al., 1997; Li et al., 1997; Rittinger et al., 1997), abolished the cellular alterations. Cells that overexpressed myr 7 carrying this point mutation (R2166M) did not exhibit any obvious alterations in cell morphology and actin filament organization (Fig. 14). Therefore, we conclude that myr 7 can also inactivate Rho in vivo.

DISCUSSION

We have cloned and characterized myr 7, a novel unconventional myosin, and RhoGAP molecule from rat. Cloning of a partial cDNA from human origin demonstrated that myr 7 is the orthologue of human myosin-IXA from which a short cDNA sequence spanning a well-conserved region in the myosin head domain has been reported previously (Bement et al., 1994). Searching the databases with the myr 7 sequence turned up several human ESTs covering different regions of the molecule. Myr 7/myosin-IXA is related to myr 5/myosin-IXB and shares with myr 5/myosin-IXB the intriguing features of an N-terminal extension, a large insertion within the myosin head domain and a zinc-binding motif and a RhoGAP region within the tail domain. However, there are also noticeable differences in that the myr 7 neck region contains six consecutive, but unevenly spaced, IQ-motifs, which represent putative light chain binding sites. In comparison, myr 5 contains four evenly spaced IQ-motifs. Recently, evidence has accumulated that the neck region in conventional myosin serves as a lever arm for force production (Block, 1996). Therefore, the irregular light chain spacing in the neck region of myr 7 as indicated by sequence analysis might alter rigidity and structure of the neck region and thereby affect force

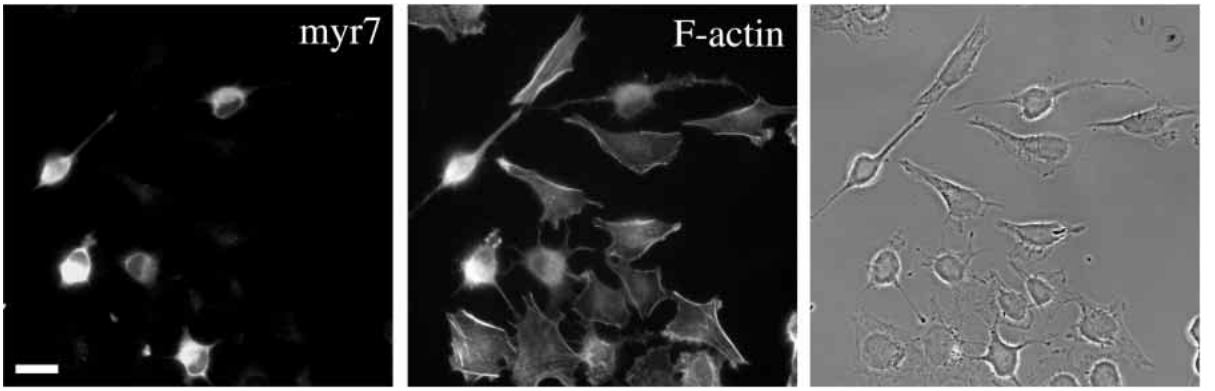

Fig. 13. Overexpression of myr 7 in HeLa cells leads to fragmentation of actin filaments and morphological changes. HeLa cells grown on coverslips were transiently transfected with myr 7 cDNA tagged with a C-terminal haemagglutinin epitope (pUHDmyr 7-HA). 36 hours after transfection, cells were fixed, permeabilized and labeled by indirect double immunofluorescence with the myr 7 antibody Tü 78 followed by a Lissamine rhodamine-coupled goat anti-rabbit antibody and with FITC-coupled phalloidin (F-actin). The labeling of the endogenous myr 7 is very weak and transfected cells are clearly distinguishable from not transfected cells. The identical field of cells is also shown by phase contrast optics (right). Bar, 10 μm.

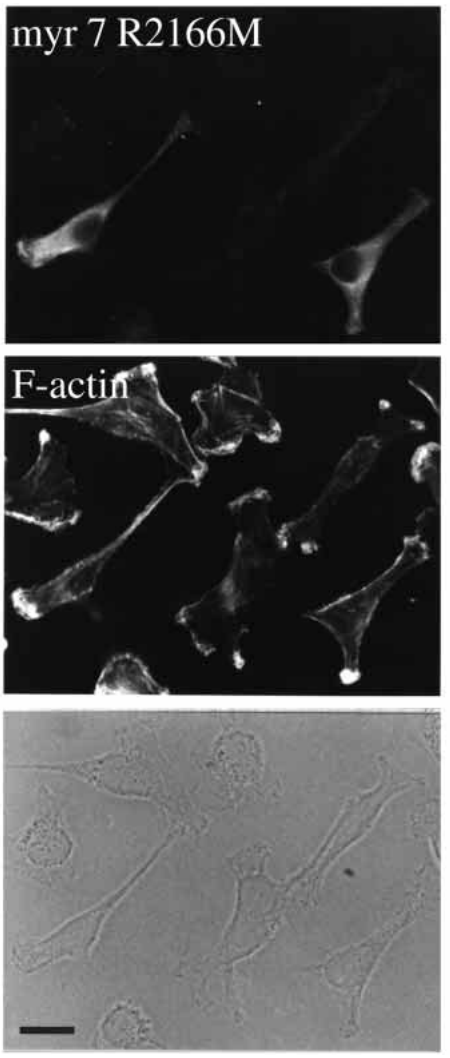

Fig. 14. The cellular alterations observed upon overexpression of myr 7 in HeLa cells are ablated by inactivation of its RhoGAP activity. HeLa cells grown on coverslips were transiently transfected with myr 7 R2166M (pUHDmyr 7-HA R2166M). 36 hours after transfection, cells were fixed, permeabilized and labeled by indirect double immunofluorescence with the myr 7 antibody Tü 78 followed by a Rhodamine-coupled goat anti-rabbit antibody and FITC-coupled phalloidin. The identical field of cells is also shown by phase contrast optics. Bar, 20 μm.

transduction. A short sequence in the C-terminal tail domain of myr 7 that is not present in myr 5 is predicted to form five heptad repeats of α-helical coiled coil structure. However, it remains to be seen whether this region can engage in homo- or heterodimer formation. In the myr 7/myosin-IXA cDNA five alternatively spliced sequences were identified. One alternatively spliced sequence is located in the 5′-noncoding region and might affect mRNA translation, transport or stability. The two alternatively spliced sequences identified in the myr 7 myosin head domain are located in positions at which class VI myosins and class IX myosins, respectively, carry insertions. These alternatively spliced sequences are likely to influence the properties or regulation of the motor domain. Because the two alternatively spliced sequences identified in the myr 7 tail domain do not reside within regions of the molecule for which a function has been described, it is currently not possible to predict what effects they might have.

Northern and immunoblot analyses of myr 7 and myr 5 expression in various tissues revealed a distinct but overlapping pattern of expression for the two proteins. Additional complexity is added by the discovery of multiple protein bands for myr 7 and myr 5. These bands might be explained in part by the different splice forms. However, expression of a single cDNA for myr 5 still results in the generation of two protein bands (R. Müller and M. Bähler, unpublished observations). Therefore, alternative modifications might exist in myr 5 and myr 7. Myr 7 is expressed at high levels in brain as opposed to myr 5, which is expressed only at low levels. Myr 7 is expressed in all brain regions and shows no striking enrichment in a particular region. It was most prominent in neuronal cell bodies and apical dendrites. This distribution suggests a general function for myr 7 in the nervous system.

Rho family members have been demonstrated to play important roles in nervous system development. Activation of Rho in mammalian neuronal cells in culture leads to the retraction of neurites (Jalink et al., 1994). Expression of a constitutively active Rac 1 in Purkinje cells of the mouse cerebellum perturbed proper axon and dendritic spine elaboration (Luo et al., 1996). In Drosophila, expression of both dominant active and negative forms of Rac 1 and Cdc42 in the nervous system caused distinct morphological defects (Luo et al., 1994). Mutations in a protein with homology to Rho family GDP-GTP exchangers also lead to aberrations in neuronal morphology (Sone et al., 1997). Another Rho family member, called mig-2, was shown to function in cell migration and axon guidance in *C. elegans* (Zipkin et al., 1997). Because myr 7 and myr 5 are expressed in the developing nervous system and because we have demonstrated that they both in vitro and in vivo negatively regulate Rho by stimulating its GTPase activity, it can be reasoned that they play an important regulatory role in nervous system development. Furthermore, Rho family members have also been implicated in exocytosis, endocytosis, actin reorganization and regulation of gene expression (for a review see Ridley, 1996), which are all important processes for neuronal function. Therefore, it seems likely that myr 7 and myr 5 are important regulators of neuronal function.

We thank Iris Kehrer and Christa Baradoy for skilful technical assistance, and Rainer Müller and Georg Kalhammer for discussion and comments on the manuscript. We acknowledge the support of Dr Manfred Schliwa, the Max-Planck Society, the Deutsche Forschungsgemeinschaft (Ba 1354/2-1/2 and SFB413) and the European Commission (contract CHRX-CT94-0652).

REFERENCES

Ahmed, S., Kozma, R., Hall, C. and Lim, L. (1995). GTPase-activating protein activity of h(a1)-chimaerin and effect of lipids. *Meth. Enzymol*. **256**, 114-124.

Ausubel, F. M., Brent, R., Kingston, R. E., Moore, D. D., Seidman, J. G., Smith, J. A. and Struhl, K. (1989). *Current Protocols in Molecular Biology*. John Wiley & Sons, Inc., New York.

Bähler, M., Kehrer, I., Gordon, L., Stöffler, H.-E. and Olsen, A. S. (1997). Physical mapping of human myosin-IXB (Myo9B), the human orthologue of the rat myosin myr 5, to chromosome 19p13.1. *Genomics* **43**, 197-109.

Bement, W. M., Hasson, T., Wirth, J. A., Cheney, R. E. and Mooseker, M.

S. (1994). Identification and overlapping expression of multiple unconventional myosin genes in vertebrate cell types. *Proc. Nat. Acad. Sci. USA* **91**, 6549-6553.

Berger, B., Wilson, D. B., Wolf, E., Tonchev, T., Milla, M. and Kim, P. S. (1995). Predicting coiled-coils by use of pairwise residue correlations. *Proc. Nat. Acad. Sci. USA* **92**, 8259-8263.

Block, S. M. (1996). Fifty ways to love your lever: Myosin motors. *Cell* **87**, 151-157.

Bradford, M. M. (1976). A rapid and sensitive method for the quantitation of microgram quantities of protein utilizing the principle of protein dye binding. *Anal. Biochem*. **72**, 248-254.

Devereux, J., Haeberli, P. and Smithies, O. (1984). A comprehensive set of sequence analysis program for the VAX. *Nucleic Acids Res*. **12**, 387-395.

Diaz-Meco, M. T., Municio, M. M., Frutos, S., Sanchez, P., Lozano, J., Sanz, L. and Moscat, J. (1996). The product of par-4, a gene induced during apoptosis, interacts selectively with the atypical isoforms of protein kinase C. *Cell* **86**, 777-786.

Jahn, R., Schiebler, W., Ouimet, C. and Greengard, P. (1985). A 38,000 dalton membrane protein (p38) present in synaptic vesicles. *Proc. Nat. Acad. Sci. USA* **82**, 4137-4141.

Jalink, K., van Corven, E. J., Hengeveld, T., Morii, N., Narumiya, S. and Moolenaar, W. H. (1994). Inhibition of lysophosphatidate- and thrombin-induced neurite retraction and neuronal cell rounding by ADP ribosylation of the small GTP-binding protein Rho. *J. Cell Biol*. **126**, 801-810.

Kalhammer, G., Bähler, M., Schmitz, F., Jöckel, J. and Block, C. (1997). Ras-binding domains: predicting function versus folding. *FEBS Lett*. **414**, 599-602.

Laemmli, U. K. (1970). Cleavage of structural proteins during assembly of the head of bacteriophage T4. *Nature* **227**, 680-685.

Li, R., Zhang, B. and Zheng, Y. (1997). Structural determinants required for the interaction between RhoGTPase and the GTPase-activating domain of p190. *J. Biol. Chem.* **272**, 32830-32835.

Luo, L., Liao, Y. J., Jan, L. Y. and Jan, Y. N. (1994). Distinct morphogenetic functions of similar small GTPases: Drosophila Drac1 is involved in axonal outgrowth and myoblast fusion. *Genes Dev.* **8**, 1787-1802.

Luo, L., Hensch, T. K., Ackermann, L., Barbel, S., Jan, L. Y. and Jan, Y. N. (1996). Differential effects of the Rac GTPase on Purkinje cell axons and dendritic trunks and spines. *Nature* **379**, 837-840.

Mott, H. R., Carpenter, J. W., Zhong, S., Ghosh, S., Bell, R. M. and Campbell, S. L. (1996). The solution structure of the Raf-1 cysteine-rich domain: a novel Ras and phospholipid binding site. *Proc. Nat. Acad. Sci. USA* **93**, 8312-8317.

Müller, R. T., Honnert, U., Reinhard, J. and Bähler, M. (1997). The rat myosin myr 5 is a GTPase activating protein for rho in vivo. Essential role of arginine 1695. *Mol. Biol. Cell* **8**, 2039-2053.

Ponting, C. P. and Benjamin, D. R. (1996). A novel family of Ras-binding domains. *Trends Biochem. Sci.* **21**, 422-425.

Reinhard, J., Scheel, A. A., Diekmann, D., Hall, A., Ruppert, C. and Bähler, M. (1995). A novel type of myosin implicated in signalling by rho family GTPases. *EMBO J.* **14**, 697-704.

Ridley, A. J. and Hall, A. (1992). The small GTP-binding protein rho regulates the assembly of focal adhesion and actin stress fibers in response to growth factors. *Cell* **70**, 389-399.

Ridley, A. J. (1996). Rho: theme and variations. *Curr. Biol.* **6**, 1256-1264.

Rittinger, K., Walker, P. A., Eccleston, J. F., Smerdon, S. J. and Gamblin, S. J. (1997). Structure at 1.65Å of RhoA and its GTPase-activating protein in complex with a transition-state analogue. *Nature* **389**, 758-762.

Schröder, R. R., Manstein, D. J., Jahn, W., Holden, H., Rayment, I., Holmes, K. C. and Spudich, J. A. (1993). Three-dimensional atomic model of F-actin decorated with Dictyostelium myosin S1. *Nature* **364**, 171-174.

Settleman, J. and Foster, R. (1995). Purification and GTPase-activating protein activity of baculovirus expressed p190. *Meth. Enzymol.* **256**, 105-113.

Sone, M., Hoshino, M., Suzuki, E., Kuroda, S., Kaibuchi, K., Nakagoshi, H., Saigo, K., Nabeshima, Y. and Hama, C. (1997). Still life, a protein in synaptic terminals of Drosophila homologous to GDP-GTP exchangers. *Science* **275**, 543-547.

Towbin, H., Staehelin, T. and Gordon, J. (1979). Electrophoretic transfer of proteins from polyacrylamide gels to nitrocellulose sheets: procedure and some applications. *Proc. Nat. Acad. Sci. USA* **76**, 4350-4354.

Uyeda, T. Q. P., Ruppel, K. M. and Spudich, J. A. (1994). Enzymatic activities correlate with chimaeric substitution at the actin-binding face of myosin. *Nature* **368**, 567-569.

Wirth, J. A., Jensen, K. A., Post, P. L., Bement, W. M. and Mooseker, M. S. (1996). Human myosin-IXb, an unconventional myosin with a chimerin-like rho/rac GTPase-activating protein domain in its tail. *J. Cell Sci.* **109**, 653-661.

Zafra, F., Hengerer, B., Leibrock, J., Thoenen, H. and Lindholm, D. (1990). Activity dependent regulation of BDNF and NGF mRNAs in the rat hippocampus is mediated by non-NMDA gutamate receptors. *EMBO J.* **9**, 3545-3550.

Zipkin, I. D., Kindt, R. M. and Kenyon, C. J. (1997). Role of a new Rho family member in cell migration and axon guidance in *C. elegans*. *Cell* **90**, 883-894.